Electrochemical Synthesis of Ceramic Materials. 3. Synthesis and Characterization of a Niobium Nitride Precursor and Niobium Nitride Powder

Travis Wade and Richard M. Crooks*

Department of Chemistry, Texas A&M University, College Station, Texas 77843-3255

Ernest Gene Garza and Douglas M. Smith

UNM/NSF Center for Micro-Engineered Ceramics, University of New Mexico, Albuquerque, New Mexico 87131

Jeffrey O. Willis and J. Yates Coulter

Superconductivity Technology Center, Los Alamos National Laboratory, Los Alamos, New Mexico 87545

Received August 24, 1993. Revised Manuscript Received November 4, 1993®

Anodic dissolution of Nb foil in an electrolyte solution containing liquid NH_3 and NH_4Br produces an insoluble precursor that can be calcined to yield phase-pure NbN. Infrared spectroscopy is consistent with a precursor having the general formula $NbX_n(NH_2)_{5-n}\cdot pNH_3$. By changing the calcination conditions, the phase of the resulting NbN powder can be varied. For example, calcining in pure Ar yields the superconducting δ-NbN phase at 600 and 800 °C but results in γ-NbN at 1000 °C. A mixed 85% Ar/15% H_2 calcining atmosphere also results in δ-NbN at 600 °C, but yields γ-NbN phases at 800 °C. When the precursor powder is calcined in NH_3 at 600, 800, or 1100 °C γ-NbN phases result, but subsequent calcining in Ar at 1450 °C yields superconducting δ-NbN (T_c = 14.75 K). The calcination ambient affects the chemical composition of the powder: in all cases more reducing conditions lower the level of Br contamination.

Introduction

In this paper we describe an electrochemical method for synthesizing a NbN precursor that yields a superconducting NbN powder when calcined at temperatures above 600 °C. To our knowledge this is the first report of an electrochemical route for preparation of a superconducting phase of NbN; the electrosynthesis is intended to complement previously reported homogeneous synthetic routes to NbN powders.[1-13]

This NbN synthesis is a new aspect of our interest in the relationship between electrochemical methods and non-oxide ceramic materials. We[14-16] and others[17-27] have previously reported electrochemical routes for synthesizing a number of different metal nitrides in either liquid NH_3 or amine-containing organic electrolyte solutions. The results of our studies indicate that there are some distinct advantages to using electrochemical methods for synthesizing non-oxide metal-nitride precursors. First, we have found that electrochemical methods afford a significant level of control over the physical characteristics of ceramic powders. For example, these powders tend to have higher surface areas and smaller particle sizes than powders produced by other routes, which is a distinct advantage for subsequent powder processing. Second, electrolytically produced powders are generally more pure than powders synthesized by alternative methods. For example we have found that all metal nitrides formed from precursors

* Author to whom correspondence should be addressed.

® Abstract published in *Advance ACS Abstracts,* December 1, 1993.

(1) Yamamoto, T.; Kikkawa, M.; Takahashi, Y.; Miyamoto, Y.; Kanamaru, F. *Physica C* **1991**, *185-189*, 2719.
(2) Kodymová, J.; Krejčí, V.; Láska, L.; Votruba, J. *Acta. Phys. Slov.* **1982**, *32*, 177.
(3) Christensen, A. N.; Fregerslev, S. *Acta. Chem. Scand. A* **1977**, *31*, 861.
(4) Maya, L. *Inorg. Chem.* **1987**, *26*, 1459.
(5) Montel, G.; Lebugle, A.; Pastor, H. In *Proc. Round Table Meet. Spec. Ceram. Electron. Electr. Eng.*; Ranachowski, J., Wlosinski, W., Wroblewska, G., Eds.; Polska Akad.; Nauk Inst. Podstawowych Probl. Tech.: Warsaw, Poland 1979; pp 7-59.
(6) Nakamura, K.; Hikita, M.; Asano, H.; Terada, A. *Jpn. J. Appl. Phys.* **1982**, *21*, 672.
(7) Ohshima, S.; Dietrich, M.; Linker, G. *J. Appl. Phys.* **1985**, *57*, 890.
(8) Lengauer, W.; Ettmayer, P. *Monatsh. Chem.* **1986**, *117*, 275.
(9) Inoue, A.; Oguchi, M.; Kim, B. G.; Misaki, H.; Masumoto, T. *Jpn. J. Appl. Phys.* **1988**, *27*, L134.
(10) Hatano, M.; Nishino, T.; Kawabe, U. *J. Vac. Sci. Technol. A* **1988**, *6*, 2381.
(11) Ezumi, H.; Endo, T.; Yamada, H.; Kuwahara, K.; Kino, T. *Thin Solid Films* **1988**, *163*, 261.
(12) Kim, S. J.; Franzen, H. F.; Lengauer, W. *J. Less-Common Met.* **1990**, *160*, 193.
(13) Gray, K. E.; Kampwirth, R. T.; Miller, D. J.; Murduck, J. M.; Hampshire, D.; Herzog, R.; Weber, H. W. *Physica C* **1991**, *174*, 340.
(14) Ross, C. B.; Wade, T.; Crooks, R. M.; Smith, D. M. *Chem. Mater.* **1991**, *3*, 768.
(15) Wade, T.; Park, J.; Garza, G.; Ross, C. B.; Smith, D. M.; Crooks, R. M. *Mater. Res. Soc. Symp. Proc.* **1992**, *271*, 857.
(16) Wade, T.; Park, J.; Garza, E. G.; Ross, C. B.; Smith, D. M.; Crooks, R. M. *J. Am. Chem. Soc.* **1992**, *114*, 9457.
(17) Maya, L. *Adv. Ceram. Mater.* **1986**, *1*, 150.
(18) Seibold, M.; Rüssel, C. *Mater. Res. Soc. Symp. Proc.* **1988**, *121*, 477.
(19) Rüssel, C.; Seibold, M. *J. Am. Ceram. Soc.* **1989**, *72*, 1503.
(20) Rüssel, C. *Chem. Mater.* **1990**, *2*, 241.
(21) Teusel, I.; Rüssel, C. *J. Mater. Sci.* **1990**, *25*, 3531.
(22) Jaschek, R.; Rüssel, C. *Surf. Coat. Technol.* **1991**, *45*, 99.
(23) Jaschek, R.; Rüssel, C. *J. Non-Cryst. Solids* **1991**, *135*, 236.
(24) Jaschek, R.; Rüssel, C. *Thin Solid Films* **1992**, *208*, 7.
(25) Rüssel, C. *J. Mater. Sci. Lett.* **1992**, *11*, 774.
(26) Rüssel, C. Zahneisen, R. *J. Electrochem. Soc.* **1992**, *139*, 2424.
(27) Distler, P.; Rüssel, C. *J. Mater. Sci.* **1992**, *27*, 133.

0897-4756/94/2806-0087$04.50/0

synthesized in liquid NH_3 contain very low levels of C and O, since these elements are never introduced into the synthesis. Impurities such as these tend to degrade electronic, photonic, and thermal properties of metal nitrides. Third, the electrochemical approach is versatile and is easily adapted to the synthesis of many pure metal nitrides besides NbN; we have used this method to synthesize AlN, TiN, MoN, Mo_2N, VN, WN, ZrN, and Zn_3N_2.[14-16,28] Fourth, our electrosynthetic approach does not result in the formation of any unrecoverable or noxious byproducts. Fifth, this method is cost-effective and easily implemented.

There are several phases of NbN, all of which are hexagonal except for δ-NbN.[29] Some of these phases, including the δ-phase, can be synthesized by modifying the calcination conditions used to process the NbN precursor. The structure of δ-NbN is B1 (NaCl) with metallic bonding character between the Nb and N atoms.[1] This phase is a solid solution with a range of stoichiometries in which the N/Nb ratio is between 0.38 and 0.98.[29] δ-NbN is also a superconductor with desirable characteristics, including high critical current density ($J_c \sim 10^5$ A/cm^2 at 4.2 K and 100 kOe), high upper critical magnetic field ($H_{c2} \sim 200$ kOe), and a relatively high superconducting transition temperature ($T_c = 17.3$ K).[2,3] Primarily because of its high J_c, NbN is a critical component of many technologically important devices including dc-superconducting quantum interference devices (SQUIDS), Josephson junctions, switches for pulsed power applications, and fusion reactor magnets.[30-34]

A number of nonelectrochemical synthetic routes for the preparation of NbN are known.[1-13] For example, direct nitridation of Nb occurs between 1500 and 1650 °C at a N_2 pressure of 4 MPa.[8] Thin films of NbN can be formed by a dc discharge over Nb metal in pure N_2.[2] Transition-metal nitrides can also be prepared by direct ammonolysis of the metal halide followed by heating of the resulting product, a process which is closely related to that reported here. For example, NbX_5 (X = Cl^-, Br^-, or I^-) undergoes direct ammonolysis in NH_3 to yield compounds of the form $NbX_n(NH_2)_{5-n}\cdot pNH_3$.[35]

The purposes of the present paper are to provide the details of this new NbN electrosynthesis, discuss the reaction pathway and compare it to that previously reported for AlN, and present characterization data for the highest T_c superconducting phase of NbN that results from calcination of the precursor powder.

Experimental Section

Precursor Synthesis. Electrochemical reactions were performed in a single-compartment, two-electrode glass cell configured for vacuum line operation.[14-16] The cell contained two 0.025-cm-thick Nb-foil electrodes (Johnson-Matthey, 99.8%), which were configured as concentric cylinders with the anode on the outside. The anode and cathode areas were 42.5 and 25.0 cm^2/side, respectively, and they were separated by about 0.5 cm. All current densities are based on the area of a single side of the electrodes. The electrodes were washed with soap and water, rinsed with deionized water and ethanol, and dried in an oven prior to electrolysis.

Reagent grade NH_4Br (Merck) was dried for 1 h in a vacuum oven at 80 °C and then enough was added to the cell to make the final concentration 0.20 M. The cell was attached to a glass, diffusion-pumped vacuum line and evacuated to a pressure of 1×10^{-4} mmHg. Anhydrous-grade NH_3 (Matheson) was purified by condensation onto Na metal at reduced pressure, followed by two freeze–pump–thaw cycles, prior to being condensed into the electrochemical cell.[14-16,36] (**Note:** NH_3 is a gas at room temperature, and it is toxic and flammable. It should be handled only in a fume hood and with extreme caution.)

Electrolyses were performed at a constant current of 0.64 A (150 A/m^2 at the anode) for 4 h using a Sorensen Model DCR 150-3B constant-current source (Raytheon Co.). The cell was immersed in a dry ice/isopropyl alcohol bath (−78 °C) during the electrolysis. The cell voltage between the electrodes was measured using a Dana Model M5900 digital multimeter and recorded as a function of time on a Kipp and Zonen Model BD-90 *X*–*Y* recorder.

Following electrolysis, NH_3 was allowed to evaporate through a Hg bubbler, and residual NH_3 was removed by evacuating the cell at 25 °C overnight. Prior to removal of the NbN precursor powder, the cell was isolated, removed from the vacuum line, and placed in a N_2-containing drybox. The precursor powder (precursor plus unreacted electrolyte) that resulted from the electrolysis was collected by scraping the cell walls with a stainless-steel spatula, and then it was transferred to quartz boats for calcination.

Calcination. The quartz boats were placed in a gastight quartz tube and then removed from the drybox. The tube was placed in a calibrated Lindberg Model 55035 tube furnace, and the precursor was exposed to flowing gas (NH_3, Ar, or 85% Ar/15% H_2 at 600 mL/min) which was purified by passing it over finely dispersed Na metal.[36] The furnace temperature was ramped to the maximum temperature noted in the text at 5 °C/min, held for 2 h, and then cooled to 25 °C at 20 °C/min. Following calcination the tube was transferred back to the drybox and the NbN product was removed for subsequent analysis.

Materials Characterization. Elemental analyses were performed by Galbraith Laboratories, Inc. (Knoxville, TN). H was analyzed using a Leco Model 800 elemental analyzer and Br was analyzed by thiosulfate titration. NbN was digested in $LiBF_4$ and Nb was determined by inductively coupled plasma spectroscopy. N was determined by ignition of the NbN powder in O_2 at 1000 °C, reduction of the resulting vapor over a Cu catalyst, and then quantitatively analyzed by thermal conductivity. Nb forms refractory oxides when heated in the presence of O_2, which makes elemental quantitation of O difficult. Since O is not intentionally introduced into the synthesis and since results obtained for AlN have indicated only low levels of O (0.7–1.4 wt %), we did not analyze for it in this study.[14-16]

FTIR analyses were performed using a N_2-purged Matheson Polaris FTIR spectrometer (2-cm^{-1} resolution, DTGS detector). Samples were prepared as KBr pellets in a N_2-containing drybox.

Surface areas were determined by N_2 adsorption at 77 K. The BET analysis employed a molecular cross-sectional area of 0.162 nm^2 and five relative pressures in the range 0.05–0.35. Prior to analysis, samples were outgassed under vacuum at 110 °C for 5 h. All measurements were made using an Autosorb-1 static volumetric analyzer.

X-ray powder diffraction spectra were obtained using a Scintag PAD V diffraction system (Cu $K\alpha_1$ line, Ni filter, Be window, and stepped scan (0.025°/step, 3 s/step)).

(28) Wade, T.; Smith, D. M.; Crooks, R. M., Texas A&M University, unpublished results.
(29) *Comprehensive Inorganic Chemistry*; Trotman-Dickerson, A. F., Ed.; Pergamon Press: New York, 1973; pp 604–607.
(30) Abe, H.; Hamasaki, K.; Ikeno, Y. *Appl. Phys. Lett.* **1992**, *61*, 1131.
(31) Hossain, M. S.; Yoshida, K.; Kudo, K.; Enpuku, K.; Yamafuji, K. *Jpn. J. Appl. Phys.* **1992**, *31*, 1033.
(32) Aoyagi, M.; Shoji, A.; Kosaka, S.; Nakagawa, H.; Takada, S. *IEEE Trans. Magn.* **1989**, *25*, 1223.
(33) Francavilla, T. L.; Peebles, D. L.; Nelson, H. H.; Claassen, J. H.; Wolf, S. A.; Gubser, D. U. *IEEE Trans. Magn.* **1987**, *MAG-2*, 1397.
(34) Capone, D. W. II; Gray, K. E.; Kampwirth, R. T.; Ho, H. L. *J. Nucl. Mater.* **1986**, *141–143*, 73.
(35) Nicholls, D. *Inorganic Chemistry in Liquid Ammonia*; Elsevier: Amsterdam, The Netherlands, 1979; pp 92–96 and references therein.
(36) Shriver, D. F.; Drezdzon, M. A. *The Manipulation of Air-Sensitive Compounds*, 2nd ed.; Wiley: New York, 1986.

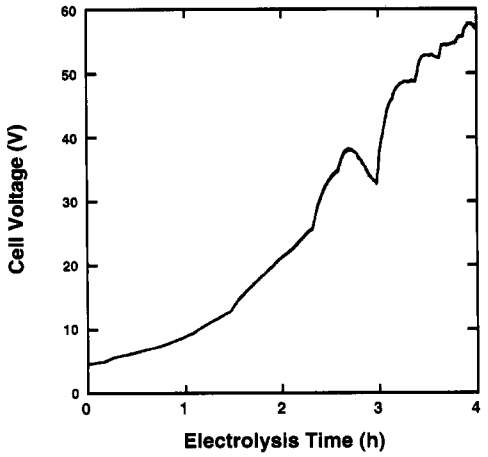

Figure 1. Cell voltage vs electrolysis time for an NbN precursor obtained by electrolyzing a 0.20 M NH_4Br solution of liquid NH_3 for 4 h at 150 A/m^2. The drop in cell voltage toward the end of the curve results from the addition of dry ice to the cooling bath. The cell volume was 80 mL.

The superconducting properties of the NbN powder were measured using a Quantum Design Model MPMS SQUID magnetometer.

Results and Discussion

Figure 1 is a plot of the cell voltage versus time during a 4-h constant-current electrolysis in the cell Nb/0.20 M NH_4Br, NH_3/Nb. Initially the cell voltage was 4.8 V, and vigorous bubbling occurred at both electrodes. Within a few minutes the solution turned pale yellow, which suggests the presence of Br_2, but after 15 min the bubbling decreased significantly. After 20 min the voltage started to rise rapidly, and we observed vigorous bubbling, especially at the cathode, once again. At the conclusion of the 4-h electrolysis, bubbles were still evident at the cathode, the solution was brown, and the cell voltage had reached nearly 60 V. A brown powder remained in the cell after the solvent was permitted to evaporate.

In our previous work,[14-16] we found that the most easily reduced species in the electrolysis cell M/NH_4Br,NH_3/M (M = Al, Ti, Mo, V, W, Zr, or Zn) is NH_4^+, and therefore we believe H_2 accounts for bubbling at the cathode, eq 1.

$$NH_4^+ + e^- \rightarrow NH_3 + {}^1/_2H_2 \quad (1)$$

$$NH_3 + e^- \rightarrow NH_2^- + {}^1/_2H_2 \quad (2)$$

$$4NH_3 \rightarrow 3NH_4^+ + 3e^- + {}^1/_2N_2 \quad (3)$$

However, if the cathode efficiency for proton reduction were equal to 1, then all of the electrolyte would be consumed within 40 min and a sharp increase in cell voltage resulting from increased cell resistance should be observed. Since the voltage rises gradually throughout the electrolysis, it seems likely that other electrode processes, which result in formation of new current-carrying ions, are operative. One likely reaction is the reduction of NH_3 (eq 2). Alternatively, or in addition, NH_4^+ formed at the anode (eq 3) will undergo reduction at the cathode (eq 1).

The presence of bubbles at the anode throughout the electrolysis suggests that eqs 3 and 4 are important electrode processes. However, only oxidation of Nb (eq 5) will yield the ceramic precursor, so it must also proceed to a significant degree.

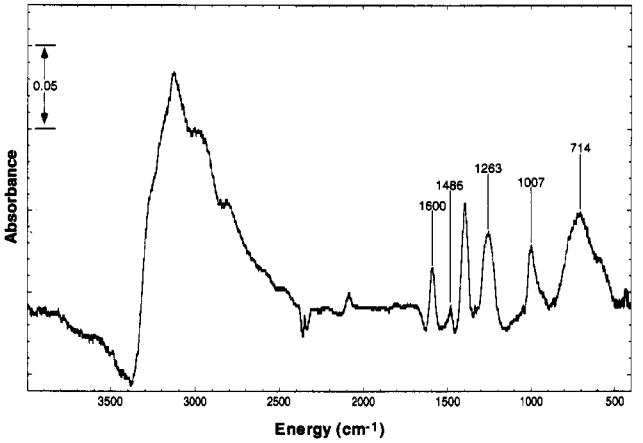

Figure 2. Transmission FTIR spectrum for the electrosynthesized NbN precursor powder before calcination.

$$Br^- \rightarrow {}^1/_2Br_2 + e^- \quad (4)$$

$$Nb \rightarrow Nb^{5+} + 5e^- \quad (5)$$

In contrast to the electrolysis of Al in liquid NH_3,[14-16] we did not observe the characteristic blue color of solvated electrons (e_s^-) during the Nb electrolysis (eq 6). Since cells

$$e^-_m \rightarrow e^-_s \quad (6)$$

configured identically to this one, except for having electrodes made from different elements, produce e_s^-, we believe their absence here results from the Nb cathode itself or their being scavenged by Nb^{5+}.

Following electrolysis the precursor powder was recovered from the cell as a brown powder. We typically obtained 2.4 g of powder at the conclusion of a 4-h electrolysis, which includes contributions from the precursor, unreacted electrolyte, and any other solid electrolysis products that might be present. The cathode weight did not change during the electrolysis, but the anode lost 0.9 g. At the current used in this experiment, 2 h would be required to oxidize 0.9 g of Nb (eq 5), which suggests that other cell components undergo oxidation at the anode thereby reducing the overall current efficiency of the electrolysis.

FTIR spectroscopic analysis of the NbN precursor reveals a number of major absorption peaks that we assign to N–H stretching and bending modes (Figure 2). Of these, all but the absorptions at 1600, 1486, 1263, 1007, 714 cm^{-1} and some of the unresolved peaks in the range 2500–3400 cm^{-1} result from NH_4Br. The presence of NH_4Br in the precursor powder at the end of the electrolysis results from ammonolysis of Nb^{5+} and salt precipitation during NH_3 evaporation (eq 7).[35]

$$NbBr_m + (2m - 2n + p)NH_3 \rightarrow NbBr_n(NH_2)_{m-n}\cdot pNH_3 + (m - n)NH_4Br \quad (7)$$

The processes corresponding to eq 3 and the reverse of eq 4 will also result in NH_4Br after NH_3 evaporation. We assign the absorptions at 1600 and 1263 cm^{-1} (Figure 2) to symmetric and degenerate NH_3 bending modes and the

Table 1. Elemental and Morphological Analyses of NbN Powders

	calcination temp (°C)		
	600	800	1000
calcination gas	85% Ar/15% H_2	Ar	Ar
phase	δ	δ	γ
elem anal. (wt %)			
Nb	81.1	77.7	84.5
N	10.1	12.9	13.3
Br	10.1	4.5	0.3
H	<0.5	<0.5	<0.5
C	<0.5	<0.5	<0.5
total	101.3	95.1	98.1
mole ratio, Nb/N	1.21	0.91	0.96
T_c (K)	10.0	13.0	9.0
BET surface area (m^2/g)	23.6	13.9	*a*
primary particle diam (nm)[40]	30.3	51.4	*a*
mean crystallite diameter (nm)[41]	4.2	13.7	*a*

[a] We did not measure these values.

absorptions at 1486, 1007, and 714 cm^{-1} to NH_2 bending modes.[37]

The infrared data suggest that the NbN precursor contains primarily NH_2 and NH_3 ligands. It is not possible for us to unambiguously assign the structure of the NbN precursor at the present time, but an empirical formula of $NbX_n(NH_2)_{5-n}\cdot pNH_3$ is consistent with all of our experimental results and the previously reported transition-metal chemistry of Nb in liquid NH_3.[35,38]

Calcination of the precursor powder at 600 °C for 2 h in 85% Ar/15% H_2 results in a 42% yield of a black powder and sublimation of a white powder, probably NH_4Br, to the end of the calcination tube.[16,38] Calcination of the precursor powder at 800 °C in 85% Ar/15% H_2 results in a 36% yield of a black powder with a metallic luster. When we calcined the precursor powder in pure Ar at 600 and 800 °C for 2 h, we obtained yields of 33% and 25%, respectively. At both temperatures a yellow/green material sublimed to the end of the tube. Transmission FTIR spectra of the NbN precursor powder following calcination at 600, 800, or 1000 °C in any of the calcining gases are featureless. This result is consistent with the presence of NbN, since the Nb–N stretching absorption will occur at an energy below the detection limit of our spectrometer.

Elemental analysis of the powder resulting from calcination at 600 °C in 85% Ar/15% H_2 reveals that it is NbN with no detectable C impurities. However, the Nb/N ratio is somewhat high and there is a significant level of Br contamination (Table 1). When we calcined the precursor powder in pure Ar at 600 °C the level of Br contamination was higher, but the NbN ratios and mass balances were lower. Although we cannot be certain of the origin of the Br contamination revealed by elemental analysis, similar results have been reported for pyrolysis of precursors formed by the ammonolysis of $NbBr_5$.[17] The missing mass and suppressed Nb/N ratio probably result from oxidation of NbN during calcination or handling, since the electrochemical method itself is inherently O-free.

X-ray analysis of the powder that results from calcination at 600 °C in 85% Ar/15% H_2 (Figure 3a) indicates broad diffraction maxima that we identify with the δ-NbN phase[39] and one small peak at about $2\theta = 30°$ that is due to spectrometer noise. Continued heating to 800 °C in

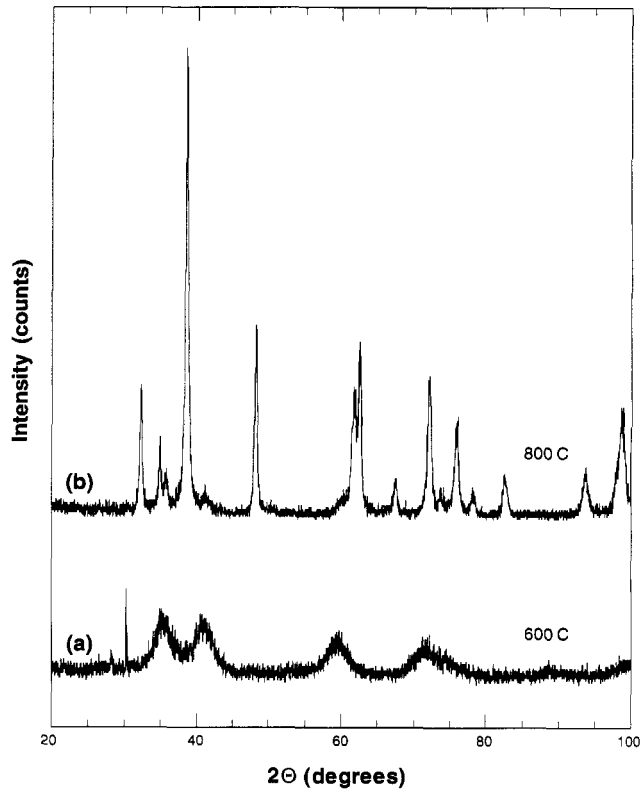

Figure 3. XRD spectra for the NbN precursor powder calcined for 2 h in flowing 85% Ar/15% H_2 (600 mL/min): (a) 600 °C; (b) 800 °C.

85% Ar/15% H_2 causes particle growth and a phase change to a mixture of γ-NbN phases (Figure 3b).[39] When the precursor powder is calcined at 800 °C in pure Ar, the δ-phase is obtained, but the powder contains more Br than when it is calcined with 15% H_2 at the same temperature: 4.5 compared to 0.36 wt %, respectively. Calcination of the precursor at 1000 °C in Ar successfully removes much of the Br impurity, but X-ray analysis indicates formation of hexagonal phases of γ-NbN under these conditions (Figure 4). Calcination in NH_3 at 600, 800, and 1100 °C results in γ-phases, but subsequent heating of the powder calcined at 1100 °C in O_2-gettered Ar at 1450 °C yields δ-NbN (Figure 5). X-ray line broadening in spectra of powders calcined at lower temperatures indicate that the NbN is nanocrystalline (Table 1), but heating to higher temperatures causes particle growth and narrower X-ray diffraction lines.

Superconductivity Analysis. We measured the zero-field cooled (ZFC, also called shielding or flux exclusion) susceptibility and field-cooled (FC, also called flux expulsion or Meissner effect) susceptibility in a field of 5 Oe between 5 and 17 K to determine the superconducting transition temperature, T_c; a parameter characterizing the width of the transition, T_c^{mid}, which is defined as the

(37) Nakamoto, K. *Infrared Spectra of Inorganic and Coordination Compounds*; Wiley: New York, 1970; p 150–159.
(38) Fowles, G. W. A.; Pollard, F. H. *J. Chem. Soc.* **1952**, 4938.
(39) *Powder Diffraction File Alphabetical Index, Inorganic Phases*; McClune, W. F., Ed.; JCPDS International Center for Diffraction Data: Swarthmore, PA, 1988. Card Numbers: δ-NbN (34-337), γ-NbN (20-801), γ-NbN (25-1361).
(40) The primary particle diameter was calculated from the measured BET surface area and skeletal or theoretical density of NbN (8.40 g/cm^3). Assuming spherical particles, $d = 6/(A\rho)$, where d is the particle diameter, A is the surface area per gram, and ρ is the density.
(41) The Scherrer equation is $D = 0.89\lambda/(B\cos\theta)$, where B is the XRD peak width at half maximum (the δ-NbN(100) peak was used for these calculations), θ is the Bragg angle (in radians), and λ is the wavelength of the incident radiation (Cu $K\alpha_1$, 1.540 60 Å). See: Cullity, B. D. *Elements of X-Ray Diffraction*; Addison-Wesley: Reading, PA, 1978; p 102.

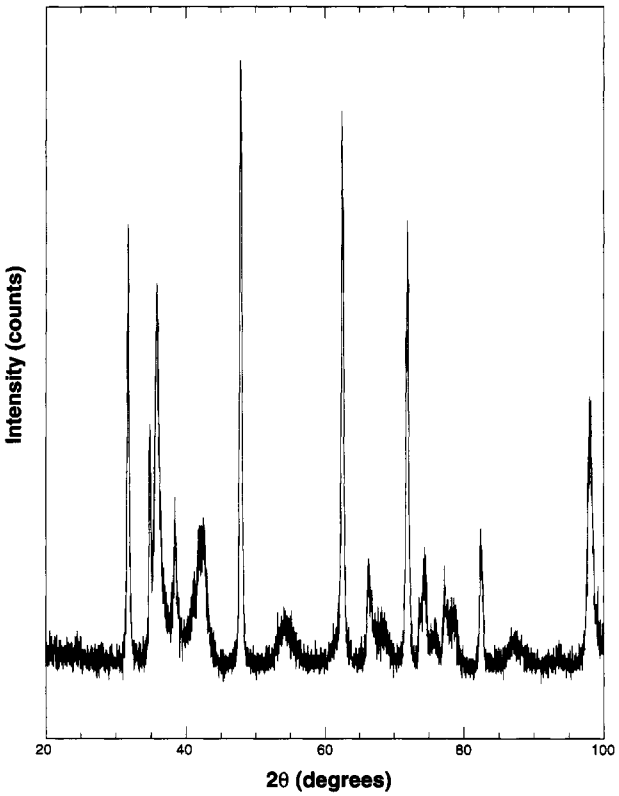

Figure 4. XRD spectrum for NbN precursor powder calcined at 1000 °C for 2 h in flowing Ar (600 mL/min).

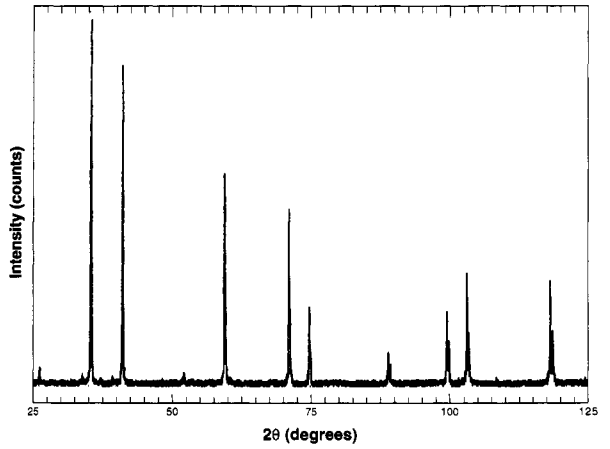

Figure 5. XRD spectrum for NbN powder calcined at 1450 °C in O_2-gettered Ar.

temperature at which the susceptibility is 50% of its low temperature value; and the volume fraction of superconducting material ($\chi_{norm}(T)$). T_c and T_c^{mid} calculated from the ZFC data are 14.75 ± 0.25 and 13.6 ± 0.08 K, respectively, for precursor calcined at 1100 °C in NH_3 and then heated to 1450 °C in Ar. Results for the FC data are the same within experimental error. We normalized the T_c data to the volume susceptibility of a perfect diamagnet ($-1/4\pi$) by correcting the measured susceptibility for the demagnetization factor (DF) of the powder particles, which we approximated as spheres with a DF of $1/3$. We also corrected the 5-Oe applied magnetic field (H) for the residual field (H_{resid}) in the superconducting magnet, which was about 0.75 Oe, and then calculated the sample volume from the measured mass and the calculated X-ray density (ρ) of 8.378 g/cm^3. The resulting relationship is given in

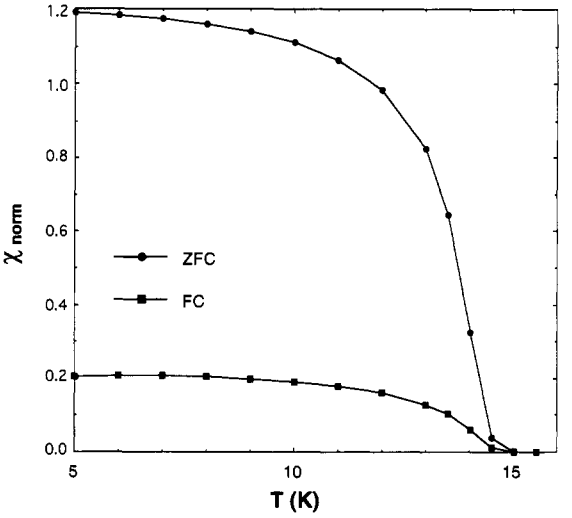

Figure 6. Zero-field-cooled (ZFC) and field-cooled (FC) normalized volume susceptibility (χ_{norm}) versus temperature for NbN precursor powder calcined at 1100 °C in NH_3 and sintered at 1450 °C in Ar. T_c = 14.75 K and H = 5 Oe.

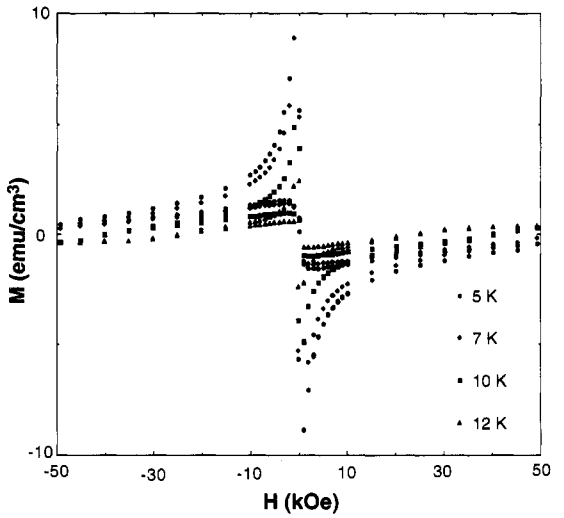

Figure 7. Magnetization loops obtained at various temperatures for fields between ±50 kOe for NbN precursor powder calcined at 1100 °C in NH_3 and sintered at 1450 °C in Ar.

eq 8, where M is the temperature-dependent magnetic moment of the sample.

$$\chi_{norm}(T) = (-4\pi M(T)[\text{emu}])\frac{(1-DF)}{(H[\text{Oe}]-H_{resid}[\text{Oe}])}\frac{\rho[\text{g/cm}^3]}{\text{mass[g]}} \quad (8)$$

The results are shown in Figure 6. The greater than 1 value for the ZFC susceptibility reflects uncertainty in one or more of the following: (1) H_{resid}; (2) the shape of the particles through the demagnetization correction; (3) shielding of small, nonsuperconducting regions within the particles. Regardless of these relatively small errors, the ZFC susceptibility is typical of results obtained for related materials. The FC susceptibility of ~0.2 is also a typical value for many superconductors. The important point is that the low-field susceptibility data confirm the high quality of the NbN powder sample.

We obtained magnetization hysteresis loops for fields between ±50 kOe (5 T) at 5, 7, 10, and 12 K (Figure 7). A field of only 1 kOe is necessary to achieve complete

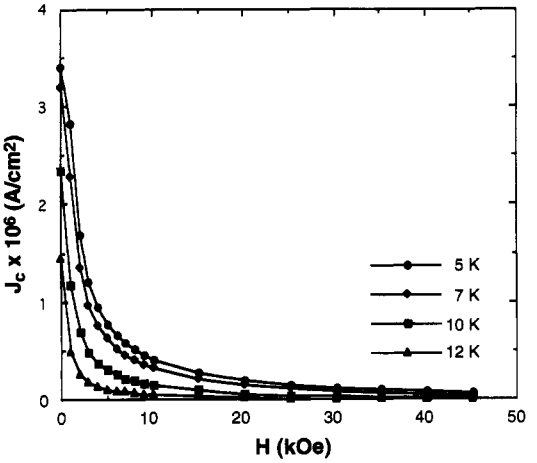

Figure 8. Magnetic field dependence of J_c for fields between 1 and 45 kOe at the temperatures shown for NbN precursor powder calcined at 1100 °C in NH_3 and sintered at 1450 °C in Ar. J_c is calculated for an estimated particle diameter of 1 μm.

penetration of magnetic flux into the sample, which reflects the small particle size of the powder. The magnetization critical current density, J_c, can be calculated from the hysteresis in the magnetization, ΔM, using the critical-state model in the Bean approximation[42] (J_c independent of H): $J_c = 30|\Delta M|/d$, where ΔM is given in emu/cm^3, d, the average particle diameter, is given in centimeters, and J_c is given in A/cm^2.

Figure 8 shows the magnetic field dependence of J_c. In the range H = 1–45 kOe, J_c is nearly proportional to $1/H$, but J_c drops off even more rapidly when $H < 1$ kOe. This behavior is similar to the weak-link behavior frequently observed in sintered, high-temperature superconductors, where it is a reflection of the poor current transfer across high-angle grain boundaries in untextured high-temperature superconductors. In the present case it may reflect current transfer between agglomerated grains of the NbN powder that breaks down in moderate fields. In general, the J_c values indicate strong pinning for this material at temperatures relatively close to T_c.

Conclusion

The electrolysis of Nb in a liquid-NH_3-containing electrolyte solution results in a NbN precursor that is similar to that formed by the ammonolysis of Nb^{5+}.[8,38] Therefore, we propose that the Nb electrode serves primarily as a source of Nb^{5+} in this electrochemical experiment. This behavior is in stark contrast to that we previously reported for the oxidation of Al in liquid NH_3 electrolyte solutions. Under identical conditions to those reported here, Al^{3+} reacts with NH_2^-, which is formed by cathodic reduction of NH_3, to form $Al(NH_2)_3$, which in turn spontaneously condenses NH_3 to yield a polymer of the form $[Al(NH_2)(NH)]_n$.

The interesting result is that identical electrolysis conditions for cells containing two different metal anodes yield completely different ceramic precursors, but both precursors yield phase-pure metal nitride powders upon calcination. In fact electrolysis of all the metals we have examined thus far yield the corresponding metal nitride when calcined above 600 °C (AlN, TiN, MoN, Mo_2N, VN, WN, ZrN, and Zn_3N_2).[28] We conclude that electrochemical methods are generally applicable to the synthesis of metal nitride powders but that different pathways are operative.

The effect of the calcining ambient on the superconductivity and purity of NbN is dramatic. For example, precursor calcined in pure Ar at 600 and 800 °C is superconducting even though a high level of Br contamination is present. Calcination at 1000 °C removes much of the Br, but it also results in a phase transition that reduces T_c. Precursor powder calcined in 85% Ar/15% H_2 results in δ-NbN at 600 °C and γ-NbN at 800 °C. Calcination in NH_3 at 600, 800, and 1100 °C yields only γ-NbN phases, but subsequent heating to 1450 °C in pure Ar returns the γ-NbN powder to the superconducting δ-phase.

Acknowledgment. This work has been partially supported by the UNM/NSF Center for Micro-Engineered Ceramics, a collaborative effort supported by NSF (CDR-8800352), Los Alamos and Sandia National Laboratories, the New Mexico Research and Development Institute, and the ceramics industry. Acknowledgment is also made to the donors of The Petroleum Research Fund, administered by the American Chemical Society, for partial support of this research. X-ray analyses were performed in the XRD Laboratory, Department of Earth and Planetary Sciences, University of New Mexico. Work at Los Alamos National Laboratory was performed under the auspices of the U.S. Department of Energy, Office of Energy Efficiency and Renewable Energy.

(42) Bean, C. P. *Phys. Rev. Lett.* **1962**, *8*, 250.